Improved near-wall accuracy for solutions of the Helmholtz equation using the boundary element method

By Y. Khalighi AND D. J. Bodony

1. Motivation and objectives

The propagation of flow-generated sound in the presence of surfaces often depends on the scattering properties of those surfaces. In the low Mach number limit and in the context of a linear acoustic theory such as that of Lighthill (1952) the process of noise prediction is divided into two steps: (i) the calculation of the sound sources generated by the flow, and (ii) the propagation of the sound. The latter stage accounts for the traveling of acoustic waves in the medium as well as the scattering of the sound due to solid objects. The propagative behavior of the environment can be fully described by the acoustic Green's function tailored to that environment's specific geometry. In the frequency domain, the Green's function is the fundamental solution of the Helmholtz equation with appropriate boundary conditions on the solid surfaces as well as a far-field radiation condition for exterior problems (Crighton 1975).

The Boundary Element Method (BEM) can be ideally employed for Helmholtz equation. It has a few inherent advantages over Finite Element and Finite Volume techniques, including the ease of applying infinite domains in exterior problems, not being subject to dissipation and dispersion error, and not requiring a volume mesh (Worbel & Aliabadi 2002).

In the BEM, the Helmholtz equation is cast into an integral equation using Green's second theorem. After surface discretization, the first step in the BEM is to numerically solve a boundary integral equation on the solid surface. In the next step the solution at any point in the volume, i.e., any point off the surface, can be calculated by a boundary quadrature formula using the results from the first step. In both steps the integral kernels exhibit singularities, or nearly so, and special attention must be paid in the evaluation of these integrals. Even if the surface solution obtained in the first step is accurate, the numerical evaluation of the surface quadrature can be inaccurate for points located within a distance of a few elements from the solid surface. The source of this inaccuracy is numerical integration of a kernel that is close to its singular point. In this work, using an asymptotic expansion of the singular kernel we present a new approach to circumvent this problem and recover the desirable order of accuracy in the vicinity of the surface.

The evaluation of the broadband noise due to the turbulent flow past an airfoil trailing edge at low Mach number is one application requiring accuracy in the Green's function obtained by quadrature. It is known that the noise generation is concentrated very close to the trailing edge (Amiet 1976; Wang & Moin 2000) where the influence of the airfoil on the sound propagation is significant. However, because of the low Mach number the acoustic wavelength is much higher than the flow scales and, as a result, the size of BEM surface mesh can be large compared to flow scales. Consequently, the major source region

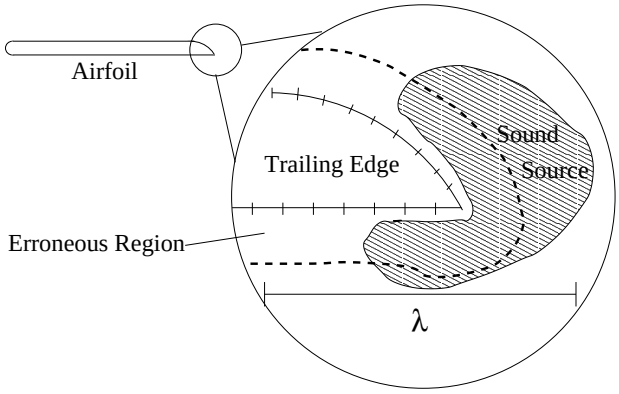

FIGURE 1. Schematic of sound source region in the vicinity of the solid surface.

can be at a distance of a few BEM surface elements and may be subject to errors due to the quadrature (see Fig. 1).

2. Basic concepts in BEM †

2.1. *Helmholtz equation, fundamental solutions, and boundary conditions*

The Helmholtz equation for a time-harmonic signal of frequency ω can be written as

$$(\nabla^2 + k^2)\phi(\mathbf{x}) = 0 \qquad \mathbf{x} \in \Omega, \tag{2.1}$$

where $k = \omega/C$ is the wavenumber and C is the constant speed of sound. Since the Helmholtz equation is presented in the frequency space ϕ is, in general, complex-valued. The fundamental solutions of the Helmholtz equation (with a source term in the form of $-\delta(\mathbf{x} - \mathbf{x_0})$) in two and three dimensions are, respectively,

$$G(\mathbf{x}, \mathbf{x_0}) = -\frac{i}{4} H_0^{(1)}(k|\mathbf{x} - \mathbf{x_0}|) \tag{2.2}$$

$$G(\mathbf{x}, \mathbf{x_0}) = -\frac{e^{ik|\mathbf{x}-\mathbf{x_0}|}}{4\pi|\mathbf{x} - \mathbf{x_0}|}, \tag{2.3}$$

where $H_0^{(1)}$ is the Hankel function of the first kind of the order zero. In the present work the derivations and results are based on an analysis of the 2-D problem but the same methodology can be applied to 3-D problems, though additional difficulties arise.

For *interior problems*, three standard boundary conditions— Dirichlet, Neumann, and Robin—can be applied on the boundary surfaces Γ_D, Γ_N, and Γ_R, respectively, where $\Gamma = \Gamma_D \cup \Gamma_N \cup \Gamma_R$ entirely bounds Ω. For *exterior problems*, in addition to previous boundary condition types for the interior surfaces, the Summerfeld radiation condition should be satisfied far from the object. The Summerfeld radiation condition can be written as

$$\lim_{r\to\infty} r\left(\frac{\partial\phi}{\partial r} + ik\phi\right) = 0 \tag{2.4}$$

and represents the propagation of sound without reflection away from the body.

† Additional details can be found in Worbel & Aliabadi (2002) and Brebbia *et al.* (1984).

2.2. *Formulation of Direct BEM Equations*

Direct boundary integral equations can be derived by applying the second Green's identity to the solution of Helmholtz equation $\phi(\mathbf{x})$ and its fundamental solution $G(\mathbf{x}, \mathbf{x_0})$. By taking the source point $\mathbf{x_0}$ on the boundary $\Gamma_\mathbf{x}$, the Helmholtz equation reduces to an integral equation on the boundary, viz,

$$c(\mathbf{x_0})\phi(\mathbf{x_0}) = \int_{\Gamma_\mathbf{x}} \frac{\partial \phi(\mathbf{x})}{\partial n} G(\mathbf{x_0}, \mathbf{x}) ds - \int_{\Gamma_\mathbf{x}} \phi(\mathbf{x}) \frac{\partial G(\mathbf{x_0}, \mathbf{x})}{\partial n} ds. \tag{2.5}$$

In this expression $c(\mathbf{x_0})$ is a geometry-dependent parameter. It varies between zero and unity and equals 1/2 if the point is on a smooth part of the boundary; at edges it is related to the angle of the joining surfaces.

If the source point $\mathbf{x_0}$ is inside the domain Ω, but not on the surface $\Gamma_\mathbf{x}$, the value of ϕ at that point can be written in terms of an integral over the surface as

$$\phi(\mathbf{x_0}) = \int_{\Gamma_\mathbf{x}} \frac{\partial \phi(\mathbf{x})}{\partial n} G(\mathbf{x_0}, \mathbf{x}) ds - \int_{\Gamma_\mathbf{x}} \phi(\mathbf{x}) \frac{\partial G(\mathbf{x_0}, \mathbf{x})}{\partial n} ds. \tag{2.6}$$

Equations 2.5 and 2.6 are the basis of the direct BEM. The method can be described as a two-step approach. In the first step, (2.5) is discretized on the surface and the integral equation is numerically *solved* for the unknowns. The type of unknown depends on the boundary condition applied on the surface, for example, on Γ_D with Dirichlet boundary condition ϕ is described and the equation is solved for $\frac{\partial \phi}{\partial n}$. In the second step the solution at any point inside the volume can be numerically *integrated* using expression (2.6).

The kernel of integrals in (2.5) and (2.6) are the free space Green's function of the Helmholtz equation and its derivative. As can be seen from (2.2) and (2.3), G and $\frac{\partial G}{\partial n}$ have singular behavior as $\mathbf{x_0}$ approaches $\mathbf{x}$. Since in (2.5) point $\mathbf{x_0}$ lies on the boundary $\Gamma_\mathbf{x}$, the kernel is singular at $\mathbf{x} = \mathbf{x_0}$. Despite the singularity these integrals exist in the sense of their Cauchy principal value and are discussed in detail in the literature (for example see Worbel & Aliabadi (2002) and Brebbia *et al.* (1984)).

Obviously, the singularity of the kernels does not take place in (2.6) as $\mathbf{x_0}$ does not lie on the surface. However, $\mathbf{x_0}$ can be very close to the surface and this causes numerical issues, which is the central focus of the current work.

3. Numerical issues in the calculation of the boundary integral

In this work we set the desirable order of accuracy as second order. We assume the boundary solution is available with at least this order of accuracy and will focus on the accuracy of the numerical quadrature for points $\mathbf{x_0}$ not on the surface. Assuming the boundary is discretized and represented by N linear elements, (2.6) can be written as

$$\phi(\mathbf{x_0}) = \sum_{i=1}^{N} \left(\int_{\Gamma_i} \frac{\partial \phi(\mathbf{x})}{\partial n} G(\mathbf{x_0}, \mathbf{x}) ds - \int_{\Gamma_i} \phi(\mathbf{x}) \frac{\partial G(\mathbf{x_0}, \mathbf{x})}{\partial n} ds \right). \tag{3.1}$$

A simple, piecewise constant representation of ϕ and $\frac{\partial \phi}{\partial n}$ is sufficient for rectangular integration, thus second order of accuracy. This can be written as

$$\phi(\mathbf{x_0}) \approx \sum_{i=1}^{N} \left(\frac{\partial \phi(\mathbf{x_i})}{\partial n} G(\mathbf{x_0}, \mathbf{x_i}) S_i - \phi(\mathbf{x_i}) \frac{\partial G(\mathbf{x_0}, \mathbf{x_i})}{\partial n} S_i \right), \tag{3.2}$$

where $\mathbf{x_i}$ and S_i are center and area of element i, respectively. In this representation the solution is approximated by N *point* monopoles and dipoles. We call this *point-wise representation*.

An alternative representation at the same order of approximation is to represent the integral by summation of *distributed* single- and double-layer acoustic potentials as

$$\phi(\mathbf{x_0}) \approx \sum_{i=1}^{N} \left(K_i \frac{\partial \phi(\mathbf{x_i})}{\partial n} - H_i \phi(\mathbf{x_i}) \right) \tag{3.3}$$

$$K_i = \int_{\Gamma_i} G(\mathbf{x_0}, \mathbf{x}) ds$$

$$H_i = \int_{\Gamma_i} \frac{\partial G(\mathbf{x_0}, \mathbf{x})}{\partial n} ds.$$

This is a *distributed representation* of the integral. The analytical expressions for H_i and K_i are not known and are not likely to exist because of the complexity of G and $\frac{\partial G}{\partial n}$ as it can be seen from (2.2) and (2.3). However, an analytical solution exists for the fundamental solution of the 2-D Laplace operator (Worbel & Aliabadi 2002).

In order to compare the accuracy of pointwise and distributed representations, a simple 2-D Laplace equation is studied. Let ψ be defined as:

$$\psi(x, y) = x \qquad -1 \leq x \leq 1, \quad -1 \leq y \leq 1. \tag{3.4}$$

The boundary of the domain is discretized into N equal elements and the exact solution is applied on the center of each element. The solution inside the domain is then calculated using different integral representations. We tested the distributed expression with 40 elements and the pointwise expression with 40, 80, and 160 elements. The results are shown in Fig. 2. Clearly, the accuracy of the pointwise expression is reduced close to the boundaries. This could be expected since the leading error term in the pointwise representation scales with h/R (where h is the size of element and $R = |\mathbf{x_0} - \mathbf{x_i}|$ as shown in Fig. 3) and that term becomes significant when $\mathbf{x_0}$ is in the vicinity region of any element. The error of the pointwise representation can be reduced by using a more accurate numerical integration, such as subdividing the closest element to smaller elements or using quadratures of higher order. Note that the error will arise as the point gets close enough to the element. As is shown in Fig. 2, the distributed formulation with 40 elements is more accurate than the pointwise expression with 160 elements in an L_∞ sense.

This observation can be problematic in acoustic applications where major sound sources are close, in terms of the acoustic wavelength, to the boundaries (see trailing edge example in Fig. 1). Here, an erroneous acoustics Green's function unphysically amplifies the noise sources close to the wall. This situation is likely to occur in the turbulent flow simulation past a solid surface where the wall normal resolution is very high ($y^+ \approx 1$). It is very expensive to use BEM elements with sizes on the order of wall units. On the other hand, an exact distributed integral formulation is not possible because of the complexity of the Green's function. An intermediate formulation, which is described in the next section, uses the asymptotic behavior of the solution in the vicinity of the near-wall elements.

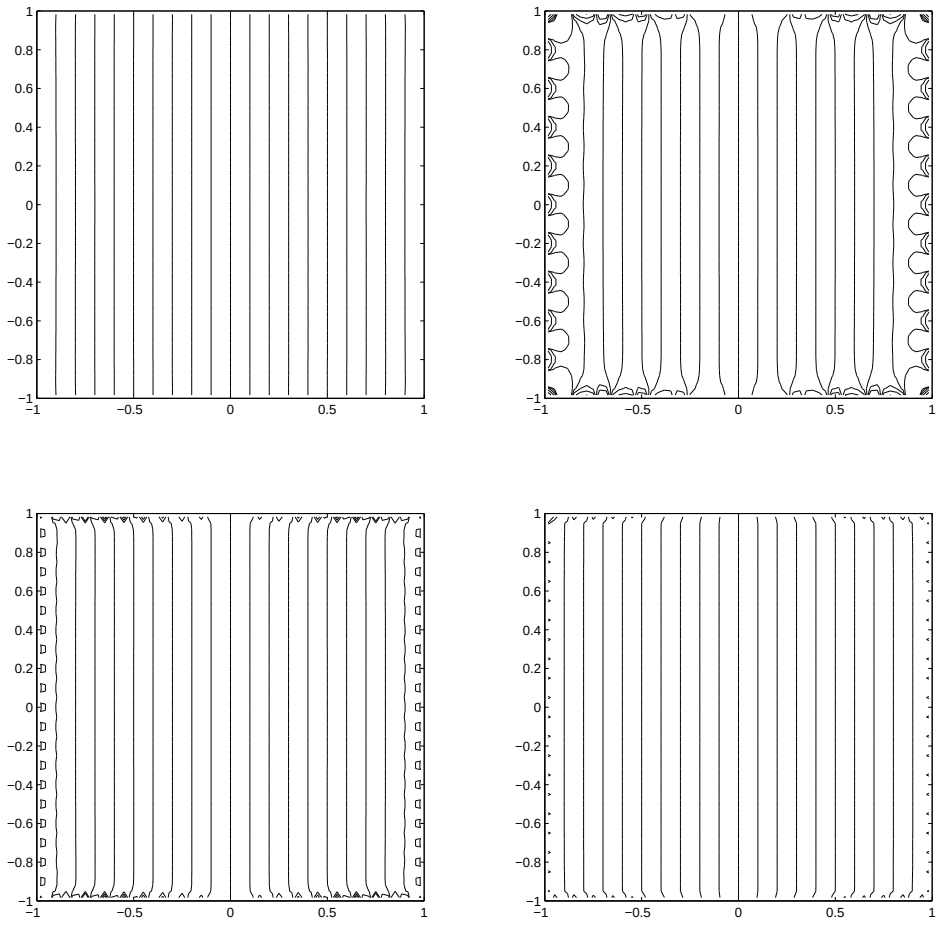

FIGURE 2. Contour levels of solution to the Laplace equation. Top left: distributed representation $N = 40$, top right: pointwise representation $N = 40$, bottom left: pointwise representation $N = 80$, bottom right: pointwise representation $N = 160$.

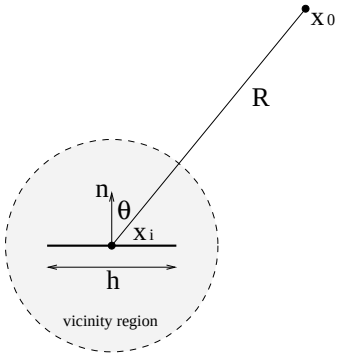

FIGURE 3. A 2-D BEM element.

4. Asymptotic expansion for 2-D BEM element

In BEM the size of boundary elements should be sufficient to resolve the wavelength $\lambda = 2\pi/k$ of the sound, implying that $h \ll \lambda$ as required by the simple elements used here. In the vicinity region of the element where R is comparable to, or smaller than, the size of element h, we have $kR \ll 1$. This observation suggests that the Helmholtz equation in this region can be approximated by the Laplace equation and that the distributed expression in its analytical form can be applied for the corresponding element. This can be verified from the asymptotic behavior of the free space Green's function for the 2-D Helmholtz equation (2.2).

From Abramowitz & Stegun (1964) the Hankel function has the following asymptotic behavior, for $|z| \ll 1$,

$$H_0^{(1)}(z) \sim \frac{2i}{\pi} \ln(z), \tag{4.1}$$

which results in the fundamental solution of the form

$$G^*(R) \sim \frac{1}{2\pi} \ln(kR) \tag{4.2}$$

$$\frac{\partial G^*(R)}{\partial R} \sim \frac{1}{2\pi R}, \tag{4.3}$$

which has the same form as the free space Green's function for the 2-D Laplace equation. Thus H_i and K_i defined in (3.4) can be approximated for the region at the vicinity of the element using the analytical expression of distributed representation. However, for points far from the element the pointwise distribution is sufficient; see Fig. 2. As a result, these two formulations can be blended using a transition function to provide a globally accurate, economical approximation for H_i and K_i. This asymptotic approximation can be written as

$$K_i \approx T(R/h) G(\mathbf{x_0}, \mathbf{x_i}) h + (1 - T(R/h)) K_i^V \tag{4.4}$$

$$H_i \approx T(R/h) \tfrac{\partial G(\mathbf{x_0}, \mathbf{x_i})}{\partial n} h + (1 - T(R/h)) H_i^V. \tag{4.5}$$

The analytical expressions for K_i^V and H_i^V are available in Appendix A. $T(\eta)$ is a transition function defined as

$$T(\eta) = 0.5(1 + \tanh(10(\eta/\alpha - 1))). \tag{4.6}$$

T and T' both vanish at $\eta = 0$. It has a smooth transition centered at $\eta = \alpha$ and becomes unity with zero derivative at sufficiently large η. Based on experience, $\alpha = 2$ provides sufficiently accurate results.

5. A test case

As a validation test case we calculate the solution for the scattering of a planar wave of wavelength $\lambda/D = 0.44$ off a solid circular cylinder, as shown in Fig. 4. The solution on the surface is calculated using second-order BEM and the solution of a point at distance d from the cylinder is calculated using the asymptotic approximation formulation of (4.4) and (4.5). The calculation is done for three different resolutions of $N = 100$, 200, and 400 elements. An analytical solution exists in the form of infinite series and is available in Appendix B. We truncate the infinite series by neglecting all terms smaller than 10^{-12} in magnitude.

The result for absolute value of the solution $|\phi|$ is shown in Fig. 5. There is desirable

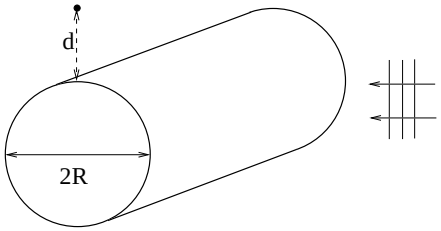

FIGURE 4. Schematic of the scattering from cylinder.

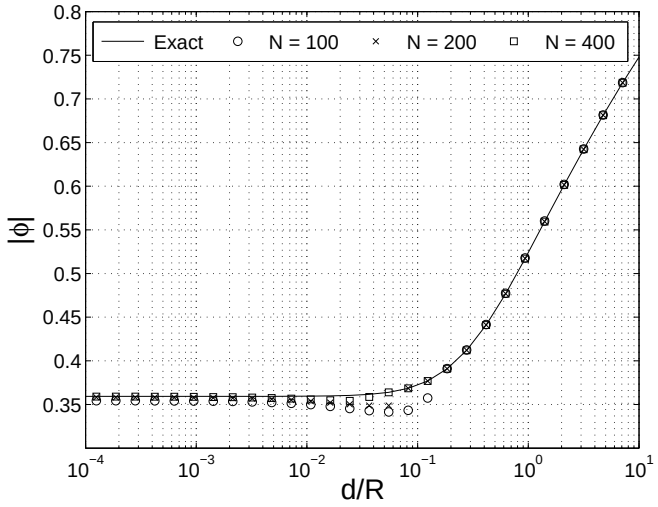

FIGURE 5. Comparison of BEM result and exact solution as the point approaches the solid surface.

agreement between the exact solution and the BEM result in the both far-field and the vicinity regions. The maximum error occurs in the transition point, as could be expected.

To assess the order of accuracy of the scheme, $(N/100)^2|\phi_{\mathrm{BEM}} - \phi_{\mathrm{exact}}|$ is plotted in Fig. 6. There it can be seen that the error curves for both asymptotic branches converge, which shows the second order of accuracy for the far-field solution and for the solution in the vicinity of the surface. Slightly better than first-order accuracy is observed in the transition region.

6. Possible extensions to 3-D problems

A key point for the implementation of 2-D asymptotic approximation is the ability to carry out the integrals analytically. Unfortunately, this is not the case in 3-D, even for very simple triangular surface elements. This problem can be remedied by making another approximation to calculate integrals in the vicinity region.

When the observer point is very close to the element, the shape of the element has very little effect. In other words, the observer does not see the edges. This suggests replacing the closest element with an element of the same area but a simpler geometry (e.g. , a circle). This method provides acceptable results (not shown) when the point is very close

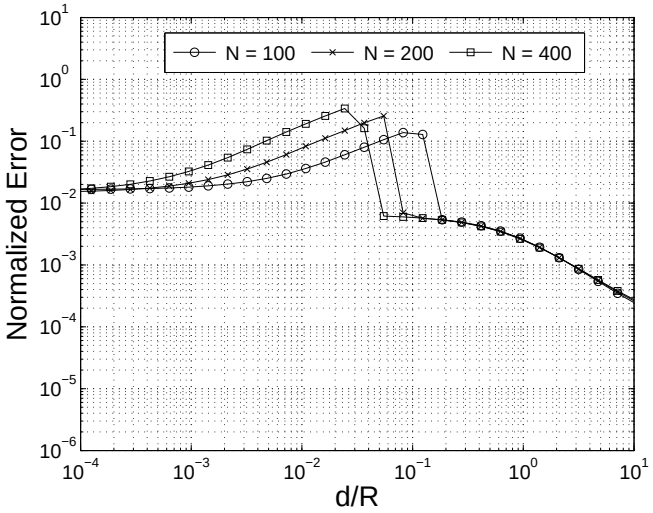

FIGURE 6. Plot of normalized error with N^2 to demonstrate the second order of accuracy.

to surface;however, it can be rather erroneous when the point is in the vicinity of the edges or far from the element.

Another technique that can be applied to both 2-D and 3-D problems is using the continuity of the solution and extrapolating the solution from the closest element. This can be written as

$$\phi \sim \phi_{boundary} - \frac{\partial \phi_{boundary}}{\partial n} d_n, \tag{6.1}$$

where d_n is normal distance between the point and the closest element. This method is very easy to implement for both 2-D and 3-D cases, but is not as accurate as using distributed representation for the vicinity region. We continue to work on the 3-D problem.

7. Summary

We have developed a new approach to accurately and efficiently calculate the boundary integrals that appear in the BEM formulation in two dimensions. It is first shown that pointwise representation of the integral can be very inaccurate close to the boundaries. Based on this observation we devised a method using the asymptotic expansion of the solution in the vicinity of elements. A simple test case was presented to show applicability of the method.

Appendix A. Analytical expressions for K_i^V and H_i^V

$$\begin{aligned} K_i^V &= \int_{element} G^* dl \qquad \text{(A 1)} \\ &= \frac{1}{4\pi}\left(b \ln\left(k^2(b^2+d^2)\right) - a \ln\left(k^2(a^2+d^2)\right) + 2d \tan^{-1}\left(\frac{4dh}{4R^2-h^2}\right) - 2h \right) \end{aligned}$$

$$H_i^V = \int_{element} \frac{\partial G^*}{\partial n} dl \qquad \text{(A 2)}$$
$$= \frac{1}{2\pi} \tan^{-1}\left(\frac{4dh}{4R^2 - h^2}\right)$$

where G^* is defined in (4.2) and a, b, and d are related to the geometry via

$$d = R\cos\theta \qquad \text{(A 3)}$$
$$a = \sqrt{R^2 + h^2/4 - Rh\sin\theta}$$
$$b = \sqrt{R^2 + h^2/4 + Rh\sin\theta}.$$

Appendix B. Exact solution of scattering from a rigid cylinder

Assume a solid cylinder with radius a is subject to a planar incident wave of wavenumber k traveling normal to the generator of the cylinder,

$$\phi_i(r,\theta) = e^{ikr\cos\theta}, \qquad \text{(B 1)}$$

where r is the polar distance from the axis and θ is measured from the direction of k.

By decomposing the solution into incident and scattered parts and separation of variables, the solution can be written as infinite series

$$\phi(r,\theta) = \phi_i + \sum_{m=0}^{\infty} A_m \cos(m\theta) H_m^{(1)}(kr), \qquad \text{(B 2)}$$

where the A_m can be calculated from

$$A_m = -2i^m \left(1 + i\frac{Y_{m-1}(ka) - Y_{m+1}(ka)}{J_{m-1}(ka) - J_{m+1}(ka)}\right)^{-1} \qquad m \neq 0 \qquad \text{(B 3)}$$

$$A_0 = -\left(1 + i\frac{Y_1(ka)}{J_1(ka)}\right)^{-1}. \qquad \text{(B 4)}$$

Acknowledgment

The work presented in this paper was supported by the Office of Naval Research.

REFERENCES

Abramowitz, M. & Stegun, I. A. 1964 *Handbook of Mathematical Functions with Formulas, Graphs, and Mathematical Tables*. New York: Dover.

Amiet, R. K. 1976 Noise due to turbulent flow past a trailing edge. *Journal of Sound Vibration* **47**, 387–393.

Brebbia, C. A., Telles, J. C. F. & Wrobel, L. C. 1984 *Boundary element techniques, Theory and application in engineering*. Berlin: Springer-Verlag.

Crighton, D. G. 1975 Basic principles of aerodynamic noise generation. *Progress in Aerospace Sciences* **16**, 31–96.

Lighthill, M. J. 1952 On Sound Generated Aerodynamically. I. General Theory. *Royal Society of London Proceedings Series A* **211**, 564–587.

Wang, M. & Moin, P. 2000 Computation of trailing-edge flow and noise using large-eddy simulation. *AIAA J.* **38**, 2201–2209.

Worbel, L. C. & Aliabadi, F. 2002 *The Boundary Element Method, Volume 1: Application in Therm-Fluids and Acoustics*. New York: John Wiley & Sons, Inc.